International Journal of Applied Glass Science, 1–8 (2016)
DOI:10.1111/ijag.12185

INTERNATIONAL JOURNAL OF
Applied Glass
SCIENCE

Evaluation of Foaming Behavior of Glass Melts by High-temperature Microscopy

Rasmus R. Petersen and Yuanzheng Yue*,†

Department of Chemistry and Bioscience, Aalborg University, DK-9220, Aalborg East, Denmark

Jakob König*

Department of Chemistry and Bioscience, Aalborg University, DK-9220, Aalborg East, Denmark

Advanced Materials Department, Jožef Stefan Institute, SI-1000, Ljubljana, Slovenia

Optical monitoring techniques can record *in situ* the size of glass samples during a dynamic heating process. This allowed us to study the sintering and expansion rate of panel glass from cathode ray tube using MnO_2 as foaming agent. We show the maximum expansion rate of glass melt foaming (*in situ* value) correlates to 50% closed porosity, and we define a universal temperature window for foaming glass melts based on the sintering–expansion curves obtained with a heating microscope. The sample size obtained at the maximum expansion rate can be used to quickly evaluate various foaming parameters such as type and concentration of foaming agent, glass composition, and particle size to obtain foam glass with high porosity and closed pores. Using this approach, we show that the foaming of bottle glass is preferentially conducted at a SiC concentration of 1 4 wt%.

Introduction

It is important that the foam glass possesses high porosity and closed pores when it is used for thermal insulation applications. However, these two features are difficult to achieve at the same time. As the porosity increases, the foam glass tends to have a higher degree of open porosity. To ensure both features, intensive optimization of foaming process is often needed. *In situ* image recording technique enables easy testing of foaming ability and allows a fast optimization of porosity. This technique has provided valuable insights into the foaming ability of glass batches[1–7] and slags.[8,9]

Few attempts have been made to systematically study the foaming ability of glass melts in a high viscosity range (~10^3 10^{12} Pa s) for the purpose of producing foam glass. Attila *et al.*[10] measured the sample height of a float glass melt using a displacement transducer to determine the temperature at which foaming begins and maximum expansion is reached. Unfortunately, these characteristic temperatures remain unrelated to the foaming conditions. Bayer and Köse[11,12] used a heating microscope to evaluate the influence of heating rate, concentration, and particle size of SiC and glass powder on the foaming ability of bottle glass.

*Member, The American Ceramic Society.
†yy@bio.aau.dk

Steiner[13] used a CCD camera to measure the vertical foam expansion of Fe_2O_3-MgO-CaO-Na_2O-Al_2O_3-SiO_2 glass melt using carbon as foaming agent, showing how heating rate and iron redox state influence the foaming ability.

In this work, we demonstrate the potential of using a heating microscope to study and optimize foaming conditions. We define and discuss characteristic temperatures from the recorded area as a function of temperature and its differential values. Based on these temperatures, we discuss the foaming ability and show a correlation between maximum expansion rate and closed porosity. The data from Bayer and Köse are revisited to demonstrate the possibility to optimize foaming agent concentration to obtain relatively high porosity and, in particular, high closed porosity.

Experimental

Milled panel glass powder from cathode ray tubes (CRT) was mixed with 7wt% MnO_2 (99%, Bie & Berntsen, Herlev, Denmark) in a porcelain jar with Al_2O_3 spheres (Ø = 3 cm). The particle sizes of glass and MnO_2 were measured with laser diffraction (LS 13320, Beckman Coulter, Brea, CA). The particle size distribution is shown in Fig. 1. The glass composition was determined with X-ray fluorescence (PW2400, PANalytical, Almelo, the Netherlands). The composition (wt%) was 61.04SiO_2-2.37Al_2O_3-7.74Na_2O-7.11K_2O-0.32MgO-0.84CaO-7.82SrO-9.66BaO-1.52ZrO_2 with a trace amount of TiO_2, Fe_2O_3, ZnO, PbO, and Sb_2O_3. The error of the measurement was <0.06 wt%.

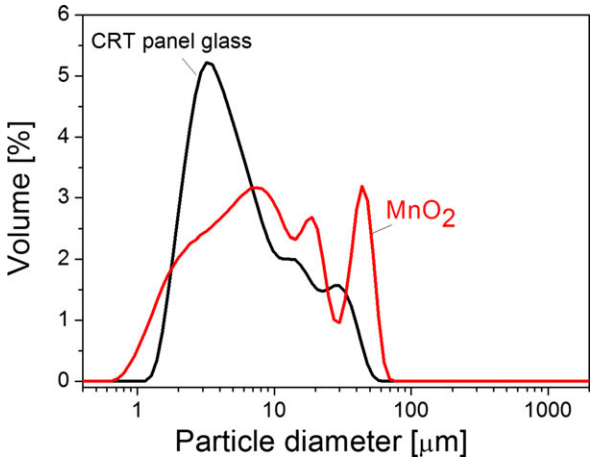

Fig. 1. Particle size distribution of CRT panel glass and MnO_2.

Powder mixture of 1.00 g was uniaxially dry pressed (40 MPa) into pellets (Ø = 13 mm, H = 4.2 mm). The pellets had a porosity of 38% ± 1% determined from the mass and dimensions of the compacted pellets. The samples were placed on alumina plates in a custom-made EM201x heating microscope (Hesse Instruments, Osterode, Germany) and heated at 10 K/min to 1173 K and then cooled to room temperature at 10 K/min. Additional foam glasses were prepared by heating the powders samples to different temperatures (T_H) between 1048 and 1149 K and then cooling them rapidly (20–30 K/min) to the glass transition temperature (T_g = 803 K). The heating microscope was equipped with a blue LED lamp, and images were recorded using a CCD b/w camera with telocentric lens. The images had a resolution of 30 μm/pixel. The thermal lag between sample and thermocouple located below the sample was determined by comparing measured temperatures with the melting or decomposition temperature of Zn (99.999%, Sigma-Aldrich, St. Louis, MO), Al (99.999%, Sigma-Aldrich), $BaCO_3$ (99.999%, Sigma-Aldrich), Ag (99.99%, Sigma-Aldrich), and Au (99.99%, Sigma-Aldrich) (see

Table I. Chemicals Used for Temperature Calibration of Heating Microscope. The Melting Temperature or Decomposition Temperature (T_{ref}) is Measured as a Sudden Change in Silhouette Area. A Pellet Consisting 1 g $BaCO_3$ Powder was Uniaxially Compacted at 40 MPa Prior Measurement

Chemical	Diameter [mm]	Length [mm]	Run no.	T_{ref} [K]	T_{meas} [K]
Zn	1	9	1	693	686
		7	2		685
		7	3		685
Al	1	6	1	933	932
		4	2		930
		10	3		930
$BaCO_3$	–	–	1	1083	1080
Ag	0.5	40	1	1235	1226
		20	2		1220
		20	3		1219
Au	0.5	8	1	1337	1337
		7	2		1333
		20	3		1337

Table I). The sudden change in the silhouette area of the metals and the pressed $BaCO_3$ during heating was attributed to the onset of melting and decomposition, respectively. The metals for calibration consisted of short (length ≈ 9–11 mm) or long wires (length ≈ 20–50 mm). $BaCO_3$ powder was uniaxially compressed with 40 MPa into a pellet (1 g) with porosity of 37%. The porosity was determined by measuring mass and dimensions of the pellet. The measured temperature (T_{meas}) of Au, $BaCO_3$ and Al agreed very well with reference temperature (T_{ref}), whereas that of Ag deviated considerably T_{ref} (Fig. 2).

The thermal gradient in radial direction of the tube furnace was determined by placing Al pieces at different positions on the alumina plate. The measurement of Al at different axial positions showed that at 15 mm away from the center (position = 0 mm) the temperature can deviate by up to 14 K when heating at 5 K/min (Fig. 3). When heating at 30 K/min, the temperature deviates by 28 K from thermocouple, which is placed in the center position below the sample holder. As foam glass expands during heating and since it is a thermal insulating medium, a temperature gradient exists throughout the sample.

The silhouette area (A) was quantified each 1.8 s with EMI 3.0.1a software (Hesse Instruments). A typical result is shown in Fig. 4 and in a Video S1. The area was normalized to the area at 423 K (A_0). The normalized area was differentiated with respect to time $r_A = d(A/A_0)/dt$ [min^{-1}] and then smoothed using "central moving average" ("adjacent-average") by averaging a moving symmetric window of 51 points. Near the boundary the window size remained symmetric but was reduced to maximum size.

The foam density (ρ_{foam}) was measured using Archimedes' principle with demineralized water. Skeletal density (ρ_{skel}) of foams and solid density (ρ_{solid}) of crushed foams were determined with He pycnometer

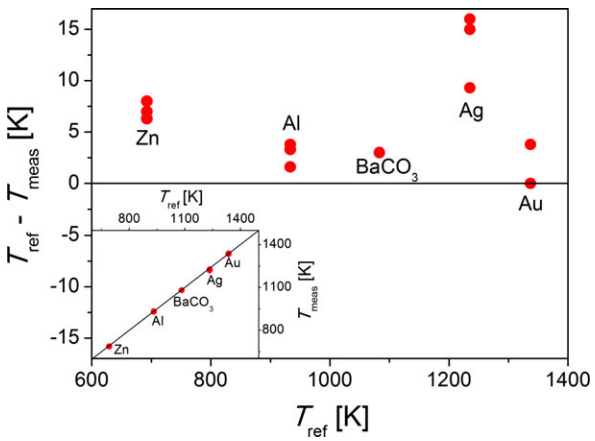

Fig. 2. Measured temperature (T_{meas}) compared with the reference melting or decomposition temperature (T_{ref}) measured at 10 K/min. The inset shows T_{ref} as a function of T_{meas}.

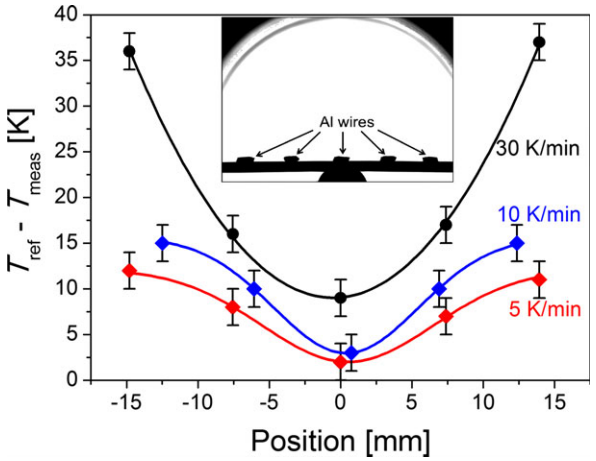

Fig. 3. Temperature distribution at 933 K in axial position at different heating rates (see legend). T_{meas} is the recorded temperature at which the area change begins and T_{ref} is the melting temperature of Al (T_{ref} = 933 K). The thermocouple is located underneath the sample in the middle of the furnace (see inset picture). The lines are guides for the eye.

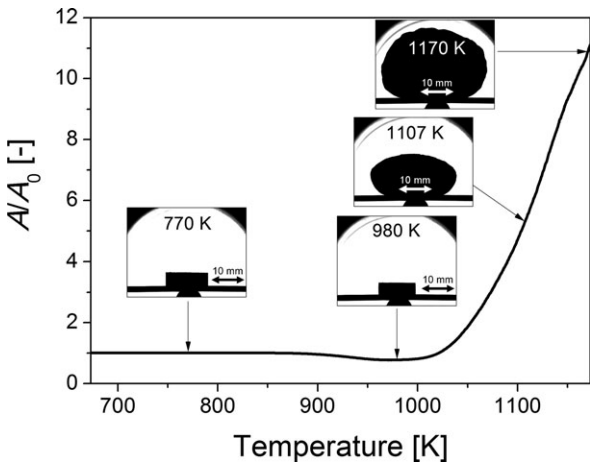

Fig. 4. A powder mixture of CRT panel glass and 7 wt% MnO_2 undergoing sintering and expansion as temperature increases. The images show the silhouettes of the body during heat treatment at 10 K/min. The silhouettes area of the sample (A) is normalized to the area (A_0) at 423 K.

(Quantachrome, Boynton Beach, Florida, USA). Here, we define the skeletal density as the density of the solid phase and the closed pores. The porosity (φ) was calculated using Eq. (1):

$$\varphi = \left(1 - \frac{\rho_{\text{foam}}}{\rho_{\text{solid}}}\right) \cdot 100\% \quad (1)$$

The closed porosity (ε) was calculated from Eq. (2):

$$\varepsilon = \frac{\rho_{\text{skel}}{}^{-1} - \rho_{\text{solid}}{}^{-1}}{\rho_{\text{foam}}{}^{-1} - \rho_{\text{solid}}{}^{-1}} \cdot 100\% \quad (2)$$

The ε data were fitted with a Boltzmann sigmoidal function Eq. (3a) to obtain a relationship between ε and treatment temperature (T_H).

$$\varepsilon(T_H) = \frac{\varepsilon_1 - \varepsilon_0}{1 + e^{(T_H - T_{50})/\Delta T}} + \varepsilon_0 \quad (3a)$$

where T_{50} is the temperature at which 50% closed porosity is reached (i.e., $\varepsilon(T_{50}) = 50\%$) and ΔT is the temperature step. ε_0 and ε_1 are asymptotic values. At low temperatures (~1050–1080 K), the sintered body has 100% closed pores, that is, $\varepsilon_1 = 100\%$. With further increase of temperature, the pores become open. Here, we assume that the foam glass becomes completely percolated at high temperatures (i.e., $\varepsilon_0 = 0\%$). T_{50} and ΔT are fitting values. We can simplify the function as:

$$\varepsilon(T_H) = \frac{1}{1 + e^{(T_H - T_{50})/\Delta T}} \quad (3b)$$

The crystalline phases in the foam glass were analyzed with X-ray diffraction (XRD) using an Empyrean diffractometer (PANalytical) with a Cu-K_α radiation source and a voltage and ampere of 45 kV and 40 mA, respectively. Measurement range was 10 to 70° (2θ) with a step size of 0.02°. The foam glasses were crushed to powder prior measurement. Crystal phases were identified by comparing peak positions and intensities with diffraction patterns in the Joint Committee on Powder Diffraction Standards (JCPDS) data files using Highscore software (PANalytical).

Results and Discussion

Characteristic Temperatures and Reproducibility

We define several characteristic temperatures from the sample area curve (A/A_0) and the derived curve ($r_A = d(A/A_0)/dt$). Sintering temperature (T_s) is defined as the onset temperature of sintering when $A/A_0 = 0.95$. Foaming temperature (T_{foam}) is defined as the temperature corresponding to the minimum area of the sample before expansion occurs. The expansion rate is zero ($r_A = 0$) at T_{foam}. The foaming onset temperature ($T_{\text{f,onset}}$) is defined as the temperature where the tangent of the sintered stage intersects with that of the starting of the expansion stage. The temperature, at which r_A reaches a maximum (Fig. 5), is defined as the maximum rate temperature ($T_{\text{r,max}}$). Each characteristic temperature can be determined within the error range of ±4 K (Table II).

The heat treatment of the mixture of glass powder and MnO_2 results in sample contraction due to glass sintering at $T_s < T < T_{\text{foam}}$ and subsequent expansion at $T > T_{\text{foam}}$ due to reduction of MnO_2 and Mn_2O_3. Pure glass powder does not foam below 1173 K.[14] After reaching maximum treatment temperature (1173 K), the foam glass cools to room temperature. During cooling, distinct drops in the A/A_0 curve appears (Fig. 5). These drops are related to bursting of very large bubbles at the sample surface.

Expansion Rate and Percolation Limit

The expansion rate (r_A [min^{-1}]) reaches a maximum value at 1129 K ($T_{\text{r,max}}$ in Fig. 5). If crystallization occurs simultaneously with the expansion, the expansion rate could be limited by the crystallization

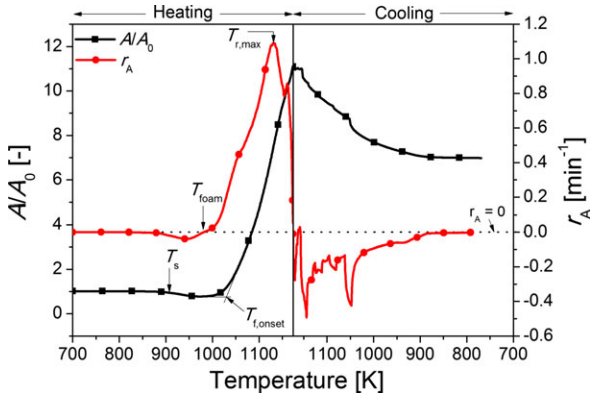

Fig. 5. Characteristic temperatures for foaming of glass melt. A/A_0 is the normalized silhouettes area and $r_A = d(A/A_0)/dt$. The characteristic temperatures are defined in the text. Heating rate is 10 K/min. The data points on the curves represent a small fraction (0.5%) of all the recorded data points.

Table II. Sintering temperature (T_s), foaming temperature (T_{foam}), foaming onset temperature ($T_{f,onset}$), and maximum rate temperature ($T_{r,max}$) of five repeating experiments. The temperatures are defined in the text.

Run number	T_s [K]	T_{foam} [K]	$T_{f,onset}$ [K]	$T_{r,max}$ [K]
1	906	977	1034	1128
2	903	971	1032	1133
3	906	975	1034	1128
4	903	972	1032	1126
5	905	972	1031	1129
Average	905 ± 2	973 ± 4	1033 ± 2	1129 ± 4

and cause the expansion rate to reach a maximum at high crystal content. The XRD results show that no crystallization occurs in the sample (Fig. 6), in accordance with our earlier studies.[14,15] Hence, the expansion ability is not affected by crystallization in this study.

During heating, the viscosity increases and bubble pressure increases with temperature. This accelerates cell wall thinning and eventually the pores will coalescence, causing a decreasing number of closed pores as the temperature increases (Fig. 7). The maximum rate could be related to the amount of closed pores, as only closed pores can contribute to foam expansion. Nucleation and growth of closed pores at high temperatures could potentially also cause foam expansion, but they have a minor effect on the foam growth.[14] Hence, the change in the expansion rate at $T_{r,max}$ could therefore be related to the pore structure undergoing a sudden change from closed to open porosity. It is not possible to measure closed porosity *in situ* with a conventional heating microscope. However, it is possible to measure the closed porosity of foam samples that are first heat-treated to T_H and subsequently cooled rapidly to T_g. The foam density (ρ_{foam}) and the closed porosity (ε) of rapidly cooled foam glasses are shown in Fig. 7.

The closed porosity is fitted to a Boltzmann sigmoidal function Eq. (3b). Fifty per cent closed porosity is reached at 1126 ± 1 K (T_{50}). In comparison, $T_{r,max}$ is 1129 ± 4 K. T_{50} is expected to be lower than the *in situ* value of $T_{r,max}$, as T_{50} is measured on foam glasses after the heat treatment. During the cooling, the pore coalescence proceeds, resulting in a slightly lower closed porosity than the real value obtained *in situ*. However, both values agree with each other within the error limit. This implies that the maximum expansion rate is reached approximately at $T_{r,max}$ when the closed porosity reaches 50%.

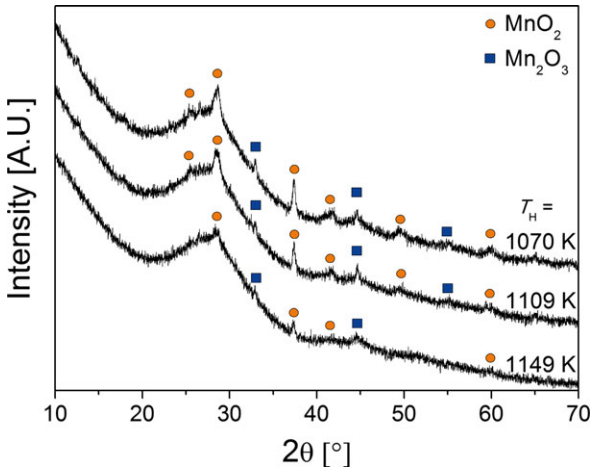

Fig. 6. X-ray diffraction patterns of foam glasses prepared from CRT panel glass using MnO_2 as the foaming agent. The foam glasses are heated to different temperatures (T_H) with 10 K/min and then cooled with 20–30 K/min to the glass transition temperature. The diffraction peaks are identified as MnO_2 (PDF no. 00-044-0141) and Mn_2O_3 phase (PDF no. 01-089-2809). The diffraction patterns are vertically shifted for clarity.

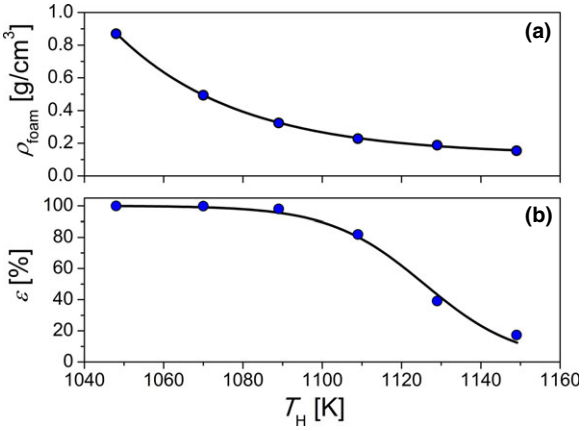

Fig. 7. (a) Foam density (ρ_{foam}) and b) closed porosity (ε) of foam glasses obtained by heating in a heating microscope to temperature (T_H) at 10 K/min and subsequently cooling the foam glass at ~20–30 K/min to the glass transition temperature (803 K). The ρ_{foam} is fitted to an exponential decay function whereas the ε data are fitted to a Boltzmann sigmoidal function Eq. (3b).

Optimal Temperature Range

Köse and Bayer[11,12] have shown with a heating microscope the influence of SiC concentration on the expansion behavior of bottle glass (Fig. 8). We use the same procedure described above to extract T_{foam}, $T_{f,onset}$, and $T_{r,max}$ from Köse's result in Fig. 8. The T_{foam}, $T_{f,onset}$, and $T_{r,max}$ are shown in Fig. 9. T_{foam} increases from 0.1 wt% to 1 wt%, but decreases again with increasing SiC concentration. $T_{r,max}$ and $T_{f,onset}$ decrease continuously with SiC concentration. By comparing Figs. 8 and 9, it is found that it is reasonable to use $T_{f,onset}$ instead of T_{foam} to define the temperature window of optimum foaming. If the glass melt is sintered into a dense body over a wider temperature range, the T_{foam} will not reflect the real start of foaming. Hence, $T_{f,onset}$ is a suitable parameter to describe the start of foaming.

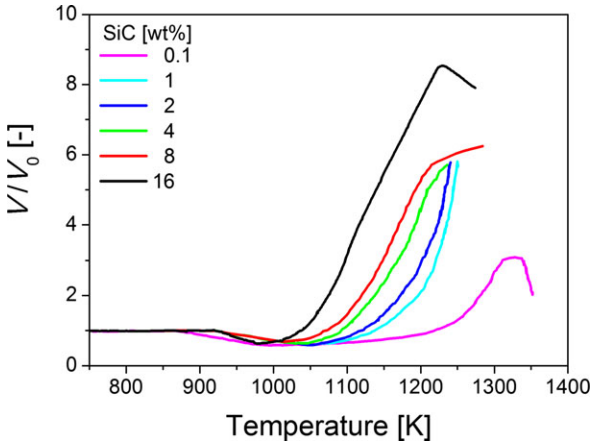

Fig. 8. Normalized sample volume (V/V_0) of bottle glass foamed with different SiC concentrations (see legend). The curves are digitized from Bayer and Köse.[11]

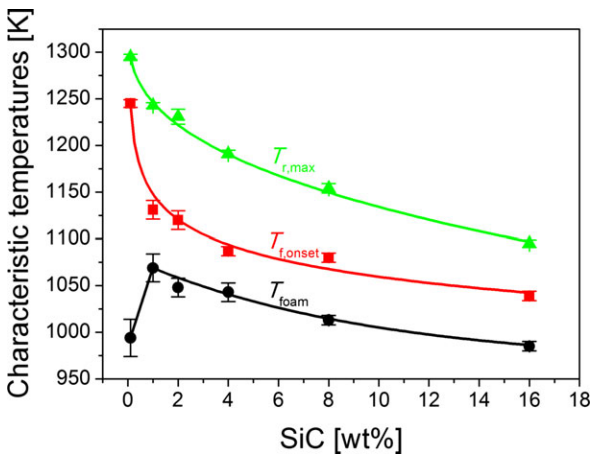

Fig. 9. Foaming temperature (T_{foam}), foaming onset temperature ($T_{f,onset}$), and maximum rate temperature ($T_{r,max}$). The characteristic temperatures are determined from Fig. 8. The lines are guides for the eye.

$T_{r,max}$ is shown above to correlate with 50% closed porosity of porous CRT panel glass, which is stable toward crystallization. For glass with low glass stability, crystallization could affect the expansion rate in two ways. First, when majority of the melt has crystallized, the expansion ability becomes limited. Second, the presence of solid can change the pore wall stability by promoting coalescence.[16] Foaming of soda-lime-silica glasses result in the formation of various crystals such as cristobalite, wollastonite, diopside, and devitrite, when mixtures of glass and foaming agent are heat-treated above 1173 K.[10,11,17–20] By studying the foaming of bottle glass using a heating microscope, Köse and Bayer[11,12] have demonstrated that crystallization could occur during expansion of foamed melt. But so far there are no literature data available, which can be used for comparing the expansion rate with crystallization degree. Prado *et al.*[21] have shown that crystallization is very limited in SLS glass powder up to 1110 K at 5 K/min. Thies and Deubener[18] have investigated the foaming of soda-lime-silica glass using SiC as foam agent by heating the glass–SiC mixture at 7.3 K/min to 1173 K, then isothermally treating it for 30 min, and finally cooling it at 2 K/min to room temperature, and thereby found ~5 vol% crystals formed after the heat treatment. As Köse and Bayer used a faster heating rate of 15 K/min compared to Thies and Deubener[18] and Prado *et al.*,[21] a lower degree of crystallization occurs during the foaming. Hence, the $T_{r,max}$ extracted from Köse and Bayer's data is likely linked to the change in closed porosity. In the following discussion, we assume therefore $T_{r,max}$ is linked to 50% closed porosity.

Köse[12] suggests that the heat treatment should not be conducted above the temperature at which maximum foam expansion is reached. Maximum foam expansion occurs at a temperature higher than the $T_{r,max}$. For most applications, foam glass should have a high degree of closed porosity. As 50% closed porosity is reached at $T_{r,max}$, the heat-treatment temperature should not exceed $T_{r,max}$. Thus, we can narrow down the temperature window for producing foam glass with closed pores, by defining the optimum temperature to

be in the range of:

$$T_{f,onst} < T < T_{r,max} \quad (4)$$

In our case, the outer part of the sample is exposed to higher temperatures (Fig. 3). In furnaces with an even temperature distribution, $T_{r,max}$ should be found at 15–17 K higher than what we find.

Applying the Percolation Limit

For many thermal insulating applications, foam glass should preferably have high porosity and closed pores. Heat treatment at $T_{f,onst} < T < T_{r,max}$ results in foam glass with >50% closed pores. Hence, the treatment temperature should reach close to $T_{r,max}$ in order to obtain low density and maintain a high degree of closed porosity. To estimate the optimum temperature and SiC concentration for foaming glass melts, we assume that any heat treatment from room temperature to $T_{r,max}$ will result in foam glasses with a high degree of closed porosity. Using this assumption, we can extract the foam expansion values ($V_{r,max}/V_0$) at $T_{r,max}$ from Fig. 8.

The results show that a maximum foam expansion (with closed pores) occurs when 2 wt% SiC is added (Fig. 10). A higher SiC concentration improves expansion ability but results in highly percolated foams. A lower SiC concentration (0.5 wt%) does not allow efficient foam expansion under dynamic heat conditions, as the temperature becomes too high before a large foam volume is reached and the pores will instead start to coalesce rapidly and eventually the foam will collapse due to the low viscosity. The results also show that the SiC concentration can potentially be tuned between 1 and 4 wt% to optimize the foam expansion and closed porosity. In foam glass industry, 1.7 wt% SiC is usually added[22] to flat, bottle, and lamp glasses[23] to produce foam glass. Hence, the optimum amount of SiC found in this work agrees well with that used by industry.

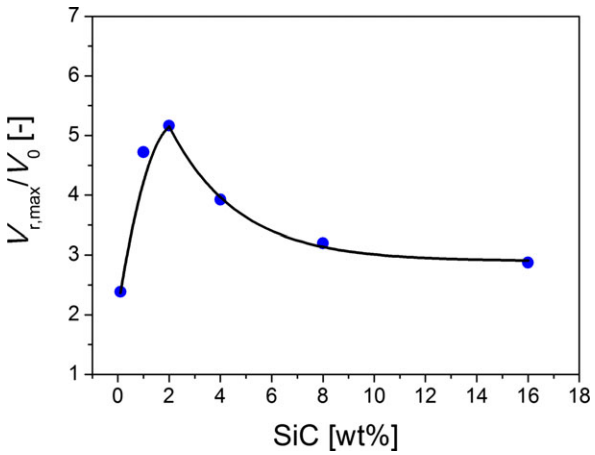

Fig. 10. Normalized foam volume ($V_{r,max}/V_0$) at maximum rate temperature ($T_{r,max}$). The $V_{r,max}/V_0$ is determined from Fig. 8. The line is a guide for the eye.

Conclusion

We have investigated the foaming ability and kinetics of glass foaming process using a heating microscope. We have demonstrated that heating microscopy is an elegant method for optimizing the processing conditions of foam glass. The sample size is obtained as a function of temperature from the silhouette area and a foaming onset temperature and a temperature of maximum expansion rate obtained from the area curves defines a universal temperature window for optimal production of foam glass with closed pores. Using the temperature of maximum expansion rate the heating microscope can also be used to optimize the concentration of foaming agent. It is expected that the heating microscope method could be extended to study the impact of type of foaming agent, particle size, and glass composition on the foaming process.

Supporting Information

Additional Supporting Information may be found in the online version of this article:

Video S1. Foaming process of the CRT glass recorded during dynamic heating by a high-temperature microscope.

References

1. S. H. Henager, P. Hrma, K. J. Swearingen, M. J. Schweiger, J. Marcial, and N. E. TeGrotenhuis, "Conversion of Batch to Molten Glass, I: Volume Expansion," *J. Non-Cryst. Solids*, 357 [3] 829–835 (2011).
2. P. Hrma, "Effect of Heating Rate on Glass Foaming: Transition to Bulk Foam," *J. Non-Cryst. Solids*, 355 [4-5] 257–263 (2009).
3. D.-S. Kim, B. C. Dutton, P. R. Hrma, and L. Pilon, "Effect of Furnace Atmosphere on E-Glass Foaming," *J. Non-Cryst. Solids* 352 [50-51] 5287–5295 (2006).

4. C. Lucktong, and P. Hrma, "Oxygen Evolution During MnO-Mn_3O_4 Dissolution in a Borosilicate Melt," *J. Am. Ceram. Soc.* 71 [5] 323–328 (1988).
5. J. der van Schaaf, and R. G. C. Beerkens, "A Model for Foam Formation, Stability, and Breakdown in Glass-Melting Furnaces," *J. Col. Int. Sci.* 295 [1] 218–229 (2006).
6. P. R. Laimböck, "Foaming of Glass Melts," Ph.D. Thesis, Technische Universiteit Eindhoven, 1998.
7. J. Kappel, R. Conradt, and H. Scholze, "Foaming Behaviour on Glass Melts," *Glastech. Ber.* 60 [6] 189–201 (1987).
8. C. F. Cooper and J. A. Kitchener, "The Foaming of Molten Silicates," *J. Iron Steel Inst.* 193 48–55 (1959).
9. Y. Zhang and R. J. Fruehan, "Effect of the Bubble Size and Chemical Reactions on Slag Foaming," *Metall. Mater. Trans. B*, 26B [4] 803–812 (1995).
10. Y. Attila, M. Güden, and A. Tasdemirci, "Foam Glass Processing Using a Polishing Glass Powder Residue," *Ceram. Int.* 39 [5] 5869–5877 (2013).
11. G. Bayer and S. Köse, "Reaction of Foaming Additives With Waste Glass Powders in the Preparation of Lightweight Materials," *Riv. della Staz. Sper. Vetro* 5 [9] 310–320 (1979).
12. S. Köse, "Untersuchungen zur Blähdynamik des Schaumglases (Study of Foam Dynamics of Foam Glass)," Ph.D. Thesis, Eidgenössischen Technischen Hochschule Zürich, 1981.
13. A. C. Steiner, "Foam Glass Production From Vitrified Municipal Waste Fly Ashes," Ph.D. Thesis, Eindhoven University, 2006.
14. R. R. Petersen, J. König, and Y.-Z. Yue, "The Mechanism of Foaming and Thermal Conductivity of Glasses Foamed With MnO_2," *J. Non-Cryst. Solids* 425 74–82 (2015).
15. J. König, R. R. Petersen, and Y.-Z. Yue, "Fabrication of Highly Insulating Foam Glass Made From CRT Panel Glass," *Ceram. Int.* 41 [8] 9793–9800 (2015).
16. A. A. Proussevitch, D. L. Sahagian, and V. A. Kutolin, "Stability of Foams in Silicate Melts," *J. Vol. Geo. Res.* 59 [1-2] 161–178 (1993).
17. J. P. Wu, A. R. Boccaccini, P. D. Lee, and R. D. Rawlings, "Thermal and Mechanical Properties of a Foamed Glass-Ceramic Material Produced From Silicate Wastes," *Proc. Eighth Eur. Soc. Glass Sci. Technol. Conf. Glass Technol.: Eur. J. Glass Sci. Technol. A* 48 [3] 133–141 (2007).
18. M. Thies and J. Deubener, "Onset of non-Newtonian Flow of Foamed Soda-Lime-Silica Glasses," *Proc. XIX Int. Congr. Glass: Glass Technol.* 43C 43–45 (2002).
19. D. U. Tulyaganov, H. R. Fernandes, S. Agathopoulos, and J. M. F. Ferreira, "Preparation and Characterization of High Compressive Strength Foams From Sheet Glass," *J. Por. Mat.* 13 [2] 133–139 (2006).
20. E. Bernardo, R. Cedro, M. Florean, and S. Hreglich, "Reutilization and Stabilization of Wastes by the Production of Glass Foams," *Ceram. Int.* 33 [6] 963–968 (2007).
21. M. O. Prado, C. Fredericci, and E. D. Zanotto, "Non-Isothermal Sintering With Concurrent Crystallization of Polydispersed Soda–Lime–Silica Glass Beads," *J. Non-Cryst. Solids* 331 [1-3] 157–167 (2003).
22. H. Pilz and J. Schweighofer, Carbon footprint of insulation materials beneath building foundations – Comparison of glass foam-granulate (Technopor) with XPS and foam glass sheet, Denkstatt GmbH, Austeria, 2008.
23. http://www.technopor.com (accessed July 15, 2015).